

Zak-OTFS for Spread Spectrum Communication

Nishant Mehrotra*, Sandesh Rao Mattu*, Robert Calderbank *Fellow, IEEE*

Abstract—An attractive feature of spread spectrum technologies such as code division multiple access (CDMA) is that it is harder to intercept or jam signals, and this feature was lost when orthogonal frequency domain modulation prevailed over CDMA in wireless standards. Legacy spread carrier waveforms are not matched to delay and Doppler shifts characteristic of 6G wireless environments, and this makes equalization very challenging. Zak-OTFS (orthogonal time frequency space) modulation is a communication framework that parameterizes the wireless channel in the delay-Doppler (DD) domain, where the parameters map directly to physical attributes of the scatterers that comprise the scattering environment. As a consequence, the channel can be efficiently acquired and equalized. The Zak-OTFS carrier is a pulse in the DD domain, and the Zak transform converts it to a pulse train modulated by a tone (pulsone) in the time domain. The pulsone waveform is localized rather than spread, and it suffers from high peak-to-average power ratio (PAPR).

We describe how to transform Zak-OTFS into a spread spectrum communication system, where the spread carrier waveforms have low PAPR and are matched to the delay and Doppler characteristics of the wireless channel. This transformation is realized by a unitary transform that is a generalization of the discrete affine Fourier transform. The transform maps a pulsone to a time domain waveform which yields a constant amplitude zero auto-correlation (CAZAC) sequence after sampling. The family of CAZAC sequences includes the Zadoff-Chu sequences incorporated in LTE and 5G-NR standards. We describe the end-to-end time-domain transceiver signal processing, comprising channel estimation and data demodulation, for the proposed system. We quantify system performance through bit error rate (BER) simulations using a six-path Vehicular-A channel model, showing that the proposed system achieves similar uncoded BER as pulsone-based Zak-OTFS, where the PAPR of each spread carrier waveform is only 3.58 dB.

Index Terms—6G, Zak-OTFS, Peak-to-Average Power Ratio, Zadoff-Chu Sequences

I. INTRODUCTION

ZAK-OTFS (orthogonal time frequency space modulation) [1], [2] is an attractive framework for communication, radar sensing, and integrated sensing and communications that processes signals in the delay-Doppler (DD) domain. The Zak-OTFS carrier waveform is a pulse in the DD domain, formally a quasi-periodic localized function with specific periods along delay and Doppler. When the channel delay spread is less than the delay period, and the channel Doppler spread is less than the Doppler period, the Zak-OTFS

This work is supported by the National Science Foundation under grants 2342690 and 2148212, in part by funds from federal agency and industry partners as specified in the Resilient & Intelligent NextG Systems (RINGS) program, and in part by the Air Force Office of Scientific Research under grants FA 8750-20-2-0504 and FA 9550-23-1-0249.

The authors are with the Department of Electrical and Computer Engineering, Duke University, Durham, NC, 27708, USA (email: {nishant.mehrotra, sandesh.rao.mattu, robert.calderbank}@duke.edu).

* denotes equal contribution.

This work may be submitted to the IEEE for possible publication. Copyright may be transferred without notice, after which this version may no longer be accessible.

Input/Output (I/O) relation changes slowly and predictably, and it is not subject to fading [1], [2]. The response to a single Zak-OTFS carrier provides an image of the the scattering environment, and can be used to predict the I/O response to all other carriers. This property makes the Zak-OTFS carrier an ideal radar waveform that can enable integrated sensing and communication in 6G wireless [2].

The Zak-OTFS carrier is realized in the time domain as a pulse train modulated by a tone (pulsone), which suffers from high peak-to-average power ratio (PAPR) [3]. It is possible to reduce PAPR significantly by applying a unitary spreading filter to pulsones in the DD domain [3]. We apply a unitary transform to pulsones in the time domain with the property that the resulting spread carrier waveforms, when sampled, give constant amplitude zero auto-correlation (CAZAC) sequences [4]–[6]. Since the transform is unitary, it enables spread carrier communication at the Nyquist rate in the presence of mobility and delay spread. The family of CAZAC sequences includes Zadoff-Chu (ZC) sequences that are widely used in LTE [7] and 5G-NR [8] wireless systems as reference signals [9], uplink random access preambles [10]–[12] and downlink synchronization signals [13]. The larger CAZAC family shares the auto-correlation and low PAPR properties [5], [6], [14] that make ZC sequences attractive.

Our contribution in this paper is as follows. We introduce a discrete generalization of the fractional Fourier transform that is unitary so that correlation properties of pulsones transfer to spread carriers without change. We then describe the end-to-end time-domain transceiver signal processing, comprising channel estimation and data demodulation, for the proposed system. We quantify system performance through bit error rate (BER) simulations using a six-path Vehicular-A channel model [15], showing that the proposed system achieves similar uncoded BER as pulsone-based Zak-OTFS, where the PAPR of each spread carrier waveform is only 3.58 dB.

Notation: x denotes a complex scalar, \mathbf{x} denotes a vector with n th entry $x[n]$, and \mathbf{X} denotes a matrix with (n, m) th entry $X[n, m]$. $(\cdot)^*$ denotes complex conjugate, $(\cdot)^H$ denotes complex conjugate transpose and $\langle \cdot, \cdot \rangle$ denotes the inner product between two vectors. Calligraphic font \mathcal{X} denotes operators or sets, with usage clear from context. \emptyset denotes the empty set. \mathbb{Z} denotes the set of integers, \mathbb{Z}_+ the set of positive integers and \mathbb{Z}_N the set of integers modulo N . (a, b) denotes the greatest common divisor of two integers a, b , $\lfloor \cdot \rfloor$ denotes the floor function, and $(\cdot)_N^{-1}$ denotes the inverse modulo N . $\delta[\cdot]$ denotes the Kronecker delta function, $\mathbf{1}_{\{\cdot\}}$ denotes the indicator function, and \mathbf{e}_n represents the standard basis vector with value 1 at location n and zero elsewhere.

II. PRELIMINARIES: ZAK-OTFS VIA PULSONES

Consider an $M \times N$ delay-Doppler (DD) grid with M delay bins (indexed by k) and N Doppler bins (indexed by

l), corresponding to width τ_p along delay and width ν_p along Doppler with $\tau_p \nu_p = 1$. The basis element corresponding to the (k_0, l_0) th DD bin, where $0 \leq k_0 \leq (M-1)$, $0 \leq l_0 \leq (N-1)$, is $\delta[k-k_0]\delta[l-l_0]$. The corresponding discrete time realization via the inverse discrete Zak transform is [16]:

$$\mathbf{x}_{(k_0, l_0)}^{(p)}[n] = \frac{1}{\sqrt{MN}} \sum_{d \in \mathbb{Z}} e^{\frac{j2\pi}{N} dl_0} \delta[n - k_0 - dM], \quad (1)$$

which is termed *pulsone* in the Zak-OTFS literature [1], [2]. The pulsone basis is orthonormal, and MN information symbols can be transmitted by modulating different pulsone:

$$\mathbf{x}_t^{(p)}[n] = \sum_{k_0=0}^{M-1} \sum_{l_0=0}^{N-1} \mathbf{X}[k_0, l_0] \mathbf{x}_{(k_0, l_0)}^{(p)}[n]. \quad (2)$$

III. SPREAD CARRIER WAVEFORMS IN ZAK-OTFS

A drawback of the pulsone basis in (1) is its high PAPR [3]. In this Section, we design spread carrier waveforms within the Zak-OTFS framework by mapping the pulsone basis to CAZACs via a unitary transform (Definition 1). In the sequel, we make use of the following two identities extensively.

Identity 1 ([17]): The sum of all N th roots of unity satisfies:

$$\sum_{n=0}^{N-1} e^{\frac{j2\pi}{N} kn} = \begin{cases} N & \text{if } k \equiv 0 \pmod{N} \\ 0 & \text{otherwise} \end{cases}.$$

Identity 2 ([17]): The quadratic Gauss sum is given by:

$$\sum_{n=0}^{N-1} e^{\frac{j2\pi}{N}(an^2+bn)} = \epsilon_N \sqrt{N} \left(\frac{a}{N}\right)_J e^{-\frac{j2\pi}{N}(4a)^{-1}b^2},$$

where N is odd, $(a, N) = 1$, $a, b \in \mathbb{Z}_+$, $\epsilon_N = 1$ if $N \equiv 1 \pmod{4}$ and $\epsilon_N = j$ if $N \equiv 3 \pmod{4}$. $\left(\frac{a}{b}\right)_J = \prod_{i=1}^k \left(\frac{a}{p_i}\right)_L^{\alpha_i}$ denotes the Jacobi symbol, which for any integer a and positive odd integer b , is the product of the Legendre symbols corresponding to the prime factors of $b = \prod_{i=1}^k p_i^{\alpha_i}$, where, for integers a and odd primes p :

$$\left(\frac{a}{p}\right)_L = \begin{cases} 0 & \text{if } a \equiv 0 \pmod{p} \\ 1 & \text{if } a \not\equiv 0 \pmod{p}, \exists x \in \mathbb{Z} : a \equiv x^2 \pmod{p} \\ -1 & \text{if } a \not\equiv 0 \pmod{p}, \nexists x \in \mathbb{Z} : a \equiv x^2 \pmod{p} \end{cases}.$$

Definition 1: The generalized discrete affine Fourier transform (GDAFT) of an MN -length sequence \mathbf{x} is given by:

$$\mathcal{F}_a \mathbf{x}[n] = \frac{1}{\sqrt{MN}} \sum_{m=0}^{MN-1} e^{\frac{j2\pi}{MN}(An^2+Bnm+Cm^2)} \mathbf{x}[m],$$

where $n \in \{0, \dots, MN-1\}$, A, B, C are co-prime to MN .

Note: The GDAFT is similar in form to the traditional discrete affine Fourier transform [18] used in signal processing.

Lemma 1: The GDAFT in Definition 1 is a unitary transform. Therefore, the inverse GDAFT is given by:

$$\mathcal{F}_a^{-1} \mathbf{x}[m] = \frac{1}{\sqrt{MN}} \sum_{n=0}^{MN-1} e^{-\frac{j2\pi}{MN}(An^2+Bnm+Cm^2)} \mathbf{x}[n].$$

Theorem 1: The GDAFT in Definition 1 maps the discrete time point pulsone given by (1) localized in the discrete DD domain at (k_0, l_0) to the CAZAC sequence:

$$\mathbf{x}_{(k_0, l_0)}^{(c)}[n] = \mathcal{F}_a \mathbf{x}_p[n] = \frac{e^{\frac{j2\pi}{MN}(An^2+Bnk_0+Ck_0^2)}}{\sqrt{MN}} \epsilon_N \left(\frac{CM}{N}\right)_J \times e^{-\frac{j2\pi}{N}(4CM)^{-1}(Bn+l_0+2Ck_0)^2}.$$

Proof: Substituting the point pulsone from (1) in Definition 1, and defining $\mathbf{x}_{(k_0, l_0)}^{(c)}[n] = \mathcal{F}_a \mathbf{x}_{(k_0, l_0)}^{(p)}[n]$,

$$\mathbf{x}_{(k_0, l_0)}^{(c)}[n] = \frac{1}{N\sqrt{M}} \sum_{m=0}^{MN-1} \sum_{d \in \mathbb{Z}} e^{\frac{j2\pi}{MN}(An^2+Bnm+Cm^2)} e^{\frac{j2\pi}{N} dl_0} \times \delta[m - k_0 - dM].$$

The delta function takes value 1 when $m = k_0 + dM$, for all $d \in \{0, \dots, N-1\}$. Therefore,

$$\mathbf{x}_{(k_0, l_0)}^{(c)}[n] = \frac{e^{\frac{j2\pi}{MN}(An^2+Bnk_0+Ck_0^2)}}{N\sqrt{M}} \sum_{d=0}^{N-1} e^{\frac{j2\pi}{N}(CMd^2+d(Bn+l_0+2Ck_0))}.$$

From Identity 2, we obtain the expression in Theorem 1. ■

Note: The expression for $\mathbf{x}_{(k_0, l_0)}^{(c)}[n]$ in Theorem 1 is equivalent to a (scaled) generalized Zadoff-Chu sequence [4], [19] (which is a member of the CAZAC family) of the form:

$$\mathbf{x}[n] = e^{\frac{j2\pi}{MN} \left(u \frac{n(n+1)}{2} + kn + \gamma \right)},$$

with parameters $u = 2(A - (4C)^{-1}B^2)$, $k = (4C)^{-1}(B^2 - 2Bl_0) - A$, $\gamma = -(k_0 l_0 + (4C)^{-1}l_0^2)$.

Corollary 1: Theorem 1 equivalently states that the GDAFT in Definition 1 maps the orthonormal pulsone basis to another orthonormal spread carrier CAZAC basis, with both bases parameterized by (k_0, l_0) , $0 \leq k_0 \leq (M-1)$, $0 \leq l_0 \leq (N-1)$.

IV. TEMPORAL SPREAD SPECTRUM PROCESSING

A. Mounting Information Symbols on Spread Carriers

From Theorem 1, we observe that analogous to (2), we can transmit MN independent information symbols by modulating the spread carrier basis formed by the CAZACs:

$$\mathbf{x}_t^{(c)}[n] = \sum_{k_0=0}^{M-1} \sum_{l_0=0}^{N-1} \mathbf{X}[k_0, l_0] \mathbf{x}_{(k_0, l_0)}^{(c)}[n]. \quad (3)$$

B. Time Domain System Model

We describe a general system model applicable to both pulsone-based and spread carrier-based Zak-OTFS. After mounting the information symbols on either basis, the time domain signal is transmitted through an *effective channel* which encompasses the effects of the linear time-varying physical channel and transmit & receive pulse shaping [2, Eq. (7)]. The received time domain signal is given by:

$$\mathbf{y}[n] = \sum_{k_0=0}^{M-1} \sum_{l_0=0}^{N-1} \sum_{k, l \in \mathbb{Z}} \mathbf{h}_{\text{eff}}[k, l] \mathbf{x}_{(k_0, l_0)}[n - k] e^{\frac{j2\pi}{MN} l(n-k)} \times \mathbf{X}[k_0, l_0] + \mathbf{w}[n], \quad (4)$$

where $\mathbf{x}_{(k_0, l_0)}[n]$ is either the (k_0, l_0) th pulse from (1) or the CAZAC from Theorem 1, $\mathbf{w}[n]$ denotes additive Gaussian noise, and $\mathbf{h}_{\text{eff}}[k, l]$ represents the effective channel.

Rewriting (4) in matrix-vector form:

$$\mathbf{y} = \mathbf{H}\mathbf{x} + \mathbf{w}, \quad (5)$$

where \mathbf{y} is the $MN \times 1$ received signal vector, \mathbf{x} is the $MN \times 1$ transmit signal vector with $\mathbf{x}[k_0 + l_0M] = \mathbf{X}[k_0, l_0]$, \mathbf{H} is the $MN \times MN$ channel matrix with $\mathbf{H}[n, k_0 + l_0M] = \sum_{k, l \in \mathbb{Z}} \mathbf{h}_{\text{eff}}[k, l] \mathbf{x}_{(k_0, l_0)}[n - k] e^{j\frac{2\pi}{MN}l(n-k)}$, and $\mathbf{w} \sim \mathcal{CN}(\mathbf{0}, \sigma^2 \mathbf{I})$ is the $MN \times 1$ vector of additive complex Gaussian noise at the receiver.

We assume transmission occurs in two stages - (i) a *pilot stage*, where a known (pilot) signal is transmitted to enable the receiver to estimate the channel, and (ii) a *data stage* where unknown data signals are transmitted, with symbol detection performed at the receiver based on channel estimates from the pilot stage. Therefore, the combined system model across the two stages can be written as:

$$\begin{bmatrix} \mathbf{y}_p & \mathbf{y}_d \end{bmatrix} = \mathbf{H} \begin{bmatrix} \mathbf{x}_p & \mathbf{x}_d \end{bmatrix} + \begin{bmatrix} \mathbf{w}_p & \mathbf{w}_d \end{bmatrix}, \quad (6)$$

where we have assumed that the channel remains constant across the two stages. For simplicity, we henceforth assume the pilot signal is the standard basis vector $\mathbf{x}_p = \mathbf{e}_{(k_p, l_p)}$, for some (k_p, l_p) , $0 \leq k_p \leq (M-1)$, $0 \leq l_p \leq (N-1)$.

C. Channel Estimation (Pilot Stage)

In the pilot stage, the receiver estimates the effective channel $\mathbf{h}_{\text{eff}}[k, l]$ by solving the maximum likelihood problem:

$$\min_{\mathbf{h}_{\text{eff}}[k, l]} \sum_{n=0}^{MN-1} \left| \mathbf{y}_p[n] - \sum_{k, l \in \mathbb{Z}} \mathbf{h}_{\text{eff}}[k, l] \mathbf{x}_{(k_p, l_p)}[n - k] \times e^{j\frac{2\pi}{MN}l(n-k)} \right|^2, \quad (7)$$

and forms an estimate of the matrix \mathbf{H} in (6) as $\hat{\mathbf{H}}[n, k_0 + l_0M] = \sum_{k, l \in \mathbb{Z}} \hat{\mathbf{h}}_{\text{eff}}[k, l] \mathbf{x}_{(k_0, l_0)}[n - k] e^{j\frac{2\pi}{MN}l(n-k)}$.

It was shown in [3] that the solution to (7) is the *cross-ambiguity function* of the received and transmitted signals:

$$\hat{\mathbf{h}}_{\text{eff}}[k, l] = \mathbf{A}_{\mathbf{y}_p, \mathbf{x}_{(k_p, l_p)}}[k, l]. \quad (8)$$

Definition 2 ([5]): The *cross-ambiguity function* of two periodic sequences $\mathbf{x}[n]$ and $\mathbf{y}[n]$ of period MN is given by:

$$\mathbf{A}_{\mathbf{y}, \mathbf{x}}[k, l] = \frac{1}{MN} \sum_{n=0}^{MN-1} \mathbf{y}[n] \mathbf{x}^*[n - k] e^{-j\frac{2\pi}{MN}l(n-k)}. \quad (9)$$

When $\mathbf{x}[n] = \mathbf{y}[n]$, $\mathbf{A}_{\mathbf{x}, \mathbf{x}}[k, l]$ is called the *self-ambiguity function* of $\mathbf{x}[n]$, which is written as $\mathbf{A}_{\mathbf{x}}[k, l]$ for brevity.

Theorem 2: The cross-ambiguity function of the GDAFT per Definition 1 of two sequences $\mathbf{x}[n]$ and $\mathbf{y}[n]$ is given by:

$$\mathbf{A}_{\mathcal{F}_a \mathbf{y}, \mathcal{F}_a \mathbf{x}}[k, l] = e^{j\frac{2\pi}{MN}(-Ak^2 + lk + CB_{MN}^{-2}(2Ak-l)^2)} \mathbf{A}_{\mathbf{y}, \mathbf{x}}[\bar{k}, \bar{l}],$$

where $\bar{k} = -B_{MN}^{-1}(2Ak - l)$, $\bar{l} = 2CB_{MN}^{-1}(2Ak - l) - Bk$.

Proof: We may express the cross-ambiguity function as the inner product of two TD sequences:

$$\begin{aligned} \mathbf{A}_{\mathbf{y}, \mathbf{x}}[k, l] &= \frac{1}{MN} \left\langle \mathbf{y}, \mathcal{D}_{k, l} \mathbf{x} \right\rangle, \\ (\mathcal{D}_{k, l} \mathbf{x})[n] &= \mathbf{x}[n - k] e^{j\frac{2\pi}{MN}l(n-k)}. \end{aligned}$$

Let \mathcal{U} and \mathcal{U}^H denote the (unitary) operators corresponding to the GDAFT and inverse GDAFT from Definition 1 and Lemma 1 respectively, such that $\mathcal{F}_a \mathbf{x}[n] = (\mathcal{U} \mathbf{x})[n]$ and $\mathcal{F}_a^{-1} \mathbf{x}[m] = (\mathcal{U}^H \mathbf{x})[m]$. Therefore, the cross-ambiguity of the GDAFT of \mathbf{y} and the GDAFT of \mathbf{x} is:

$$\begin{aligned} \mathbf{A}_{\mathcal{F}_a \mathbf{y}, \mathcal{F}_a \mathbf{x}}[k, l] &= \frac{1}{MN} \left\langle \mathcal{U} \mathbf{y}, \mathcal{D}_{k, l} \mathcal{U} \mathbf{x} \right\rangle \\ &= \frac{1}{MN} \left\langle \mathbf{y}, \mathcal{U}^H \mathcal{D}_{k, l} \mathcal{U} \mathbf{x} \right\rangle, \end{aligned}$$

where the final expression follows from the fact that the operator \mathcal{U} is unitary. Note that by definition:

$$\begin{aligned} (\mathcal{D}_{k, l} \mathcal{U} \mathbf{x})[n] &= \frac{1}{\sqrt{MN}} \sum_{m=0}^{MN-1} e^{j\frac{2\pi}{MN}(A(n-k)^2 + B(n-k)m)} \\ &\quad \times e^{j\frac{2\pi}{MN}(Cm^2 + l(n-k))} \mathbf{x}[m]. \end{aligned}$$

Therefore,

$$\begin{aligned} (\mathcal{U}^H \mathcal{D}_{k, l} \mathcal{U} \mathbf{x})[m] &= \frac{1}{MN} \sum_{n=0}^{MN-1} e^{-j\frac{2\pi}{MN}(An^2 + Bnm + Cm^2 - l(n-k))} \\ &\quad \times \sum_{m'=0}^{MN-1} e^{j\frac{2\pi}{MN}(A(n-k)^2 + B(n-k)m' + Cm'^2)} \mathbf{x}[m'] \\ &= \frac{1}{MN} \sum_{m'=0}^{MN-1} \mathbf{x}[m'] e^{j\frac{2\pi}{MN}(Ak^2 - Cm^2 - lk - Bkm')} \\ &\quad \times e^{j\frac{2\pi}{MN}Cm'^2} \sum_{n=0}^{MN-1} e^{j\frac{2\pi}{MN}((Bm' + l - 2Ak - Bm)n)}. \end{aligned}$$

From Identity 1, the inner summation over n vanishes unless $(Bm' + l - 2Ak - Bm) \equiv 0 \pmod{MN}$, when it takes value MN . Therefore, $Bm' = Bm + (2Ak - l) + fMN \implies m' = m + B_{MN}^{-1}(2Ak - l) + B_{MN}^{-1}fMN$ for $f \in \mathbb{Z}$. Therefore:

$$\begin{aligned} (\mathcal{U}^H \mathcal{D}_{k, l} \mathcal{U} \mathbf{x})[m] &= \mathbf{x}[m + B_{MN}^{-1}(2Ak - l) + B_{MN}^{-1}fMN] \\ &\quad \times e^{j\frac{2\pi}{MN}(Ak^2 - Cm^2 - lk - k(Bm + (2Ak - l) + fMN))} \\ &\quad \times e^{j\frac{2\pi}{MN}(C(m + B_{MN}^{-1}(2Ak - l) + B_{MN}^{-1}fMN)^2)} \\ &= \mathbf{x}[m + B_{MN}^{-1}(2Ak - l)] e^{j\frac{2\pi}{MN}(Ak^2 - Cm^2 - lk)} \\ &\quad \times e^{j\frac{2\pi}{MN}(-k(Bm + (2Ak - l)) + C(m + B_{MN}^{-1}(2Ak - l))^2)}, \end{aligned}$$

where the final expression follows from the MN -periodicity of $\mathbf{x}[n]$ and the MN -th roots of unity. On substituting we obtain the desired result. \blacksquare

Lemma 2: The channel estimate via (8) equals $\mathbf{h}_{\text{eff}}[k, l]$ when the *channel support*, $\mathcal{S} = \{(k, l) : \mathbf{h}_{\text{eff}}[k, l] \neq 0\}$, satisfies the *crystallization condition*:

$$\mathcal{S} \cap \left(\bigcup_{n, m \neq (0, 0)} (\mathcal{S} + (k'_{n, m}, l'_{n, m})) \right) = \emptyset,$$

where, for spread carrier-based Zak-OTFS with GDAFT parameters A, B, C , $k'_{n,m} = -2CB_{MN}^{-1}nM - B_{MN}^{-1}mN$, $l'_{n,m} = (B - 4ACB_{MN}^{-1})nM - B_{MN}^{-1}2AmN$. For pulsone-based Zak-OTFS, $k'_{n,m} = nM$, $l'_{n,m} = mN$.

Proof: By definition, in the absence of noise, we have:

$$\begin{aligned}\widehat{\mathbf{h}}_{\text{eff}}[k', l'] &= \mathbf{A}_{\mathbf{y}_p, \mathbf{x}_{(k_p, l_p)}}[k', l'] \\ &= \sum_{k, l \in \mathbb{Z}} \mathbf{h}_{\text{eff}}[k, l] \mathbf{A}_{\mathbf{x}_{(k_p, l_p)}}[k' - k, l' - l] e^{\frac{j2\pi}{MN}l(k' - k)}.\end{aligned}$$

For pulsone-based Zak-OTFS, we know from [3] that:

$$\mathbf{A}_{\mathbf{x}_{(k_p, l_p)}^{(p)}}[k, l] = \sum_{n, m \in \mathbb{Z}} e^{\frac{j2\pi}{N}nl_p} e^{-\frac{j2\pi}{M}mk_p} \delta[k - nM] \delta[l - mN].$$

Therefore,

$$\begin{aligned}\widehat{\mathbf{h}}_{\text{eff}}[k', l'] &= \sum_{k, l \in \mathbb{Z}} \mathbf{h}_{\text{eff}}[k, l] \mathbf{A}_{\mathbf{x}_{(k_p, l_p)}^{(p)}}[k' - k, l' - l] e^{\frac{j2\pi}{MN}l(k' - k)} \\ &= \mathbf{h}_{\text{eff}}[k', l'] + \sum_{(n, m) \neq (0, 0)} e^{\frac{j2\pi}{N}n(l_p + l')} e^{-\frac{j2\pi}{M}mk_p} \\ &\quad \times \mathbf{h}_{\text{eff}}[k' - nM, l' - mN].\end{aligned}$$

Therefore, $\widehat{\mathbf{h}}_{\text{eff}}[k', l'] = \mathbf{h}_{\text{eff}}[k', l']$ if the channel support satisfies the condition in the Theorem statement.

For spread carrier-based Zak-OTFS, from Theorem 2:

$$\mathbf{A}_{\mathbf{x}_{(k_p, l_p)}^{(c)}}[k, l] = e^{\frac{j2\pi}{MN}(-Ak^2 + lk + CB_{MN}^{-2}(2Ak - l)^2)} \mathbf{A}_{\mathbf{x}_{(k_p, l_p)}^{(p)}}[\bar{k}, \bar{l}],$$

where $\bar{k} = -B_{MN}^{-1}(2Ak - l)$, $\bar{l} = 2CB_{MN}^{-1}(2Ak - l) - Bk$.

On substituting the expression for $\mathbf{A}_{\mathbf{x}_{(k_p, l_p)}^{(p)}}[k, l]$,

$$\begin{aligned}\mathbf{A}_{\mathbf{x}_{(k_p, l_p)}^{(c)}}[k, l] &= e^{\frac{j2\pi}{MN}(-Ak^2 + lk + CB_{MN}^{-2}(2Ak - l)^2)} \sum_{n, m \in \mathbb{Z}} e^{\frac{j2\pi}{N}nl_p} \\ &\quad \times e^{-\frac{j2\pi}{M}mk_p} \delta[\bar{k} - nM] \delta[\bar{l} - mN].\end{aligned}$$

The delta functions in terms of (\bar{k}, \bar{l}) may be equivalently expressed in terms of (k, l) by solving the 2×2 linear equations $\bar{k} = -B_{MN}^{-1}(2Ak - l) = nM$, $\bar{l} = 2CB_{MN}^{-1}(2Ak - l) - Bk = mN$ for (k, l) . The solution gives:

$$\begin{aligned}\mathbf{A}_{\mathbf{x}_{(k_p, l_p)}^{(c)}}[k, l] &= e^{\frac{j2\pi}{MN}(-Ak^2 + lk + CB_{MN}^{-2}(2Ak - l)^2)} \sum_{n, m \in \mathbb{Z}} e^{\frac{j2\pi}{N}nl_p} \\ &\quad \times e^{-\frac{j2\pi}{M}mk_p} \delta[k - k'_{n,m}] \delta[l - l'_{n,m}],\end{aligned}$$

where $(k'_{n,m}, l'_{n,m})$ are as defined in the Theorem statement. Substituting into the expression for $\widehat{\mathbf{h}}_{\text{eff}}[k', l']$ gives the desired condition for $\widehat{\mathbf{h}}_{\text{eff}}[k', l'] = \mathbf{h}_{\text{eff}}[k', l']$ to hold. ■

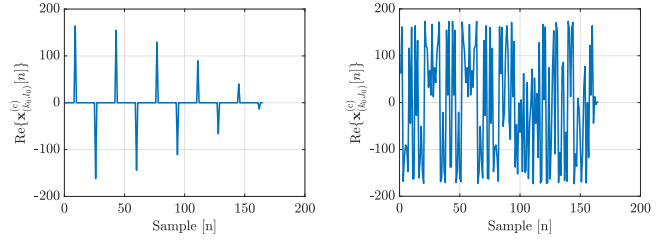
D. Data Detection (Data Stage)

In the data stage, the receiver performs data detection via the minimum mean squared error (MMSE) estimator [20]:

$$\widehat{\mathbf{x}} = (\widehat{\mathbf{H}}^H \widehat{\mathbf{H}} + \sigma^2 \mathbf{I})^{-1} \widehat{\mathbf{H}}^H \mathbf{y}. \quad (10)$$

TABLE I: Power-delay profile of Veh-A channel model

Path index i	1	2	3	4	5	6
Delay τ_i (μs)	0	0.31	0.71	1.09	1.73	2.51
Relative power (dB)	0	-1	-9	-10	-15	-20



(a) Pulsone basis element. (b) Spread carrier basis element.

Fig. 1: Time-domain waveforms of pulsone and spread carrier basis elements corresponding to $(k_0, l_0) = ((M+1)/2, (N+1)/2)$. The former has a PAPR of 15.1 dB, whereas the latter has a PAPR of 3.58 dB. Note that only the real part of a portion of the entire waveform is shown.

V. NUMERICAL RESULTS

We simulate the system model in (6) for the pulsone and spread carrier systems with parameters $M = 17, N = 19$, Doppler period $\nu_p = 30$ KHz. The effective channel $\mathbf{h}_{\text{eff}}[k, l]$ in (4) corresponds to sampling the continuous channel [1]–[3]:

$$\begin{aligned}\mathbf{h}_{\text{eff}}[k, l] &= \mathbf{h}_{\text{eff}}\left(\tau = \frac{k\tau_p}{M}, \nu = \frac{l\nu_p}{N}\right), \\ \mathbf{h}_{\text{eff}}(\tau, \nu) &= \mathbf{w}_{\text{RX}}(\tau, \nu) *_{\sigma} \mathbf{h}_{\text{phy}}(\tau, \nu) *_{\sigma} \mathbf{w}_{\text{TX}}(\tau, \nu),\end{aligned} \quad (11)$$

where $*_{\sigma}$ denotes twisted convolution¹. We assume sinc transmit pulse shaping and matched filtering at the receiver [1]–[3]:

$$\begin{aligned}\mathbf{w}_{\text{TX}}(\tau, \nu) &= \sqrt{BWT} \text{sinc}(BW\tau) \text{sinc}(T\nu), \\ \mathbf{w}_{\text{RX}}(\tau, \nu) &= e^{j2\pi\nu\tau} \mathbf{w}_{\text{TX}}^*(-\tau, -\nu),\end{aligned} \quad (12)$$

where $BW = M\nu_p, T = N\tau_p$. The physical channel in (11), $\mathbf{h}_{\text{phy}}(\tau, \nu) = \sum_{i=1}^P h_i \delta(\tau - \tau_i) \delta(\nu - \nu_i)$, corresponds to a 3GPP-compliant $P = 6$ path Vehicular-A (Veh-A) channel model [15] with significant mobility and delay spread, whose power-delay profile is shown in Table I. The Doppler of each path is simulated as $\nu_i = \nu_{\text{max}} \cos(\theta_i)$, with θ_i uniformly distributed in $[-\pi, \pi]$ and $\nu_{\text{max}} = 815$ Hz denoting the maximum channel Doppler spread. Note that the delay and Doppler of each path in the model is *fractional* in nature. For the spread carrier basis, we choose the GDAFT parameters $A = 3, B = 5, C = 7$ such that the crystallization condition in Lemma 2 holds. The transmitted data symbols \mathbf{x}_d in (6) are chosen from 4-QAM (quadrature amplitude modulation).

A. Peak-to-Average Power Ratio (PAPR) Comparison

Fig. 1 plots the time-domain waveforms of the pulsone and spread carrier basis elements with a sinc transmit pulse shaping filter. Due to the constant amplitude property of CAZACs, the latter has 11.5 dB lower PAPR than the former.

¹ $a(\tau, \nu) *_{\sigma} b(\tau, \nu) = \iint a(\tau', \nu') b(\tau - \tau', \nu - \nu') e^{j2\pi\nu'(\tau - \tau')} d\tau' d\nu'$.

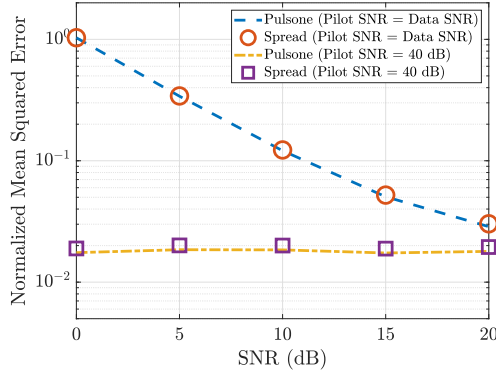


Fig. 2: Normalized mean squared error in channel estimation is the same for pulsone- and spread carrier-based Zak-OTFS.

B. Channel Estimation Performance

Fig. 2 plots the normalized mean squared error (NMSE) in channel estimation via the cross-ambiguity expression in (8) for pulsone- and spread carrier-based Zak-OTFS. We consider two cases - (i) equal signal-to-noise ratio (SNR) in the pilot and data stages in (6), and (ii) with 40 dB pilot SNR. The NMSE of the former reduces with increasing pilot SNR and approaches the NMSE of the latter at 40 dB SNR. In both cases, the NMSEs match for pulsones and spread carriers, i.e., the systems are equivalent. Note that channel estimates only need to be accurate enough (not perfect) for data detection.

C. Data Detection Performance

Fig. 3 plots the bit error rate (BER) curves for pulsone- and spread carrier-based Zak-OTFS for both cases described in Section V-B as well as perfect channel knowledge. The BER with 40 dB pilot SNR is equivalent to that with perfect channel knowledge. The BER curve for equal pilot and data SNR approaches the other curves with increasing SNR. In all cases, the BERs match for pulsones and spread carriers.

VI. CONCLUSION

In this paper, we proposed a spread spectrum communication system using Zak-OTFS by transforming high-PAPR pulsones to low-PAPR CAZAC sequences via a unitary transformation. We demonstrated the equivalence of both systems via bit error rate simulations with a six-path Vehicular-A channel model. Future work will further explore the application of the proposed spread spectrum Zak-OTFS in secure communication, radar sensing, and integrated sensing & communication.

REFERENCES

- [1] S. K. Mohammed, R. Hadani, A. Chockalingam, and R. Calderbank, "OTFS—a mathematical foundation for communication and radar sensing in the delay-Doppler domain," *IEEE BITS the Information Theory Magazine*, vol. 2, no. 2, pp. 36–55, 2022.
- [2] —, "OTFS—predictability in the delay-Doppler domain and its value to communication and radar sensing," *IEEE BITS the Information Theory Magazine*, vol. 3, no. 2, pp. 7–31, 2023.
- [3] M. Ubadah, S. K. Mohammed, R. Hadani, S. Kons, A. Chockalingam, and R. Calderbank, "Zak-OTFS for integration of sensing and communication," *arXiv preprint arXiv:2404.04182*, 2024.

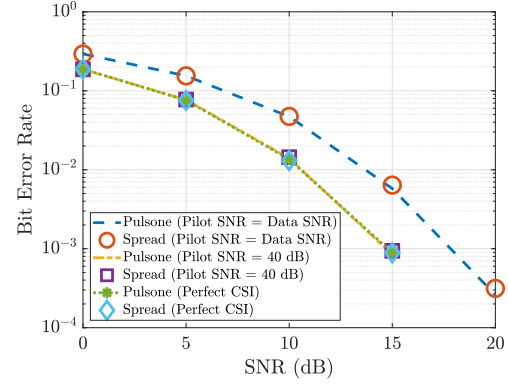


Fig. 3: Bit error rate curves showing the equivalence of data detection with pulsone- and spread carrier-based Zak-OTFS.

- [4] N. Mehrotra, S. R. Mattu, and R. Calderbank, "Zak-OTFS for Mutually Unbiased Sensing and Communication," 2025. [Online]. Available: <https://arxiv.org/abs/2503.23540>
- [5] J. J. Benedetto, I. Konstantinidis, and M. Rangaswamy, "Phase-Coded Waveforms and Their Design," *IEEE Signal Processing Magazine*, vol. 26, no. 1, pp. 22–31, 2009.
- [6] J. J. Benedetto, K. Cordwell, and M. Magsino, "CAZAC sequences and Haagerup's characterization of cyclic N-roots," *New Trends in Applied Harmonic Analysis, Volume 2: Harmonic Analysis, Geometric Measure Theory, and Applications*, pp. 1–43, 2019.
- [7] 3GPP, "3rd Generation Partnership Project; Technical Specification - LTE; Evolved Universal Terrestrial Radio Access (E-UTRA); Physical channels and modulation," 3GPP, Tech. Rep. TS 36.211 V9.1.0 (2010-04), 2010.
- [8] —, "3rd Generation Partnership Project; Technical Specification - 5G; NR; Physical channels and modulation," 3GPP, Tech. Rep. TS 38.211 V16.2.0 (2020-07), 2020.
- [9] B. Ghimire, E. Eberlein, and M. Alawieh, "Reference Signal Enhancement in 5G for Extended Coverage in Multi-User Scenarios," in *2022 IEEE 96th Vehicular Technology Conference (VTC2022-Fall)*, 2022, pp. 1–6.
- [10] M. Hyder and K. Mahata, "Zadoff-Chu Sequence Design for Random Access Initial Uplink Synchronization in LTE-Like Systems," *IEEE Transactions on Wireless Communications*, vol. 16, no. 1, pp. 503–511, 2017.
- [11] S. R. Mattu, I. A. Khan, V. Khammammetti, B. Dabak, S. K. Mohammed, K. Narayanan, and R. Calderbank, "Delay-Doppler signal processing with Zadoff-Chu sequences," *arXiv preprint arXiv:2412.04295*, 2024.
- [12] P. Agostini, J.-F. Chamberland, F. Clazzer, J. Dommel, G. Liva, A. Munari, K. Narayanan, Y. Polyanskiy, S. Stanczak, and Z. Utkovski, "Evolution of the 5G new radio two-step random access towards 6G unsourced MAC," *arXiv preprint arXiv:2405.03348*, 2024.
- [13] M. M. U. Gul, X. Ma, and S. Lee, "Timing and Frequency Synchronization for OFDM Downlink Transmissions Using Zadoff-Chu Sequences," *IEEE Transactions on Wireless Communications*, vol. 14, no. 3, pp. 1716–1729, 2015.
- [14] J. G. Andrews, "A Primer on Zadoff Chu Sequences," *arXiv preprint arXiv:2211.05702*, 2022.
- [15] ITU-R M.1225, "Guidelines for evaluation of radio transmission technologies for IMT-2000," *International Telecommunication Union Radio communication*, 1997.
- [16] H. Bolcskei and F. Hlawatsch, "Discrete Zak transforms, polyphase transforms, and applications," *IEEE Transactions on Signal Processing*, vol. 45, no. 4, pp. 851–866, 1997.
- [17] M. Murty and S. Pathak, "Evaluation of the quadratic Gauss sum," *Evaluation*, vol. 86, no. 1-2, 2017.
- [18] S.-C. Pei and J.-J. Ding, "Closed-Form Discrete Fractional and Affine Fourier Transforms," *IEEE Transactions on Signal Processing*, vol. 48, no. 5, pp. 1338–1353, 2000.
- [19] S. Budisin, "Decimation generator of zadoff-chu sequences," in *Sequences and Their Applications – SETA 2010*, C. Carlet and A. Pott, Eds. Berlin, Heidelberg: Springer Berlin Heidelberg, 2010, pp. 30–40.
- [20] D. Tse and P. Viswanath, *Fundamentals of wireless communication*. Cambridge university press, 2005.